

Article

Influence of Water-Binder Ratio on the Mechanical Strength and Microstructure of Arch Shell Interface Transition Zone

Tao He ¹, Weiheng Xiang ^{2,*}, Jian Zhang ³, Cheng Hu ^{2,*}, Gaozhan Zhang ⁴ and Bin Kou ⁵

¹ Poly Changda Engineering Co., Ltd., Guangzhou 510620, China; h9943v@163.com

² Collaborative Innovation Center for Exploration of Nonferrous Metal Deposits and Efficient Utilization of Resources, Guilin University of Technology, Guilin 541004, China

³ Anhui Construction Engineering Building Materials Co., Ltd., Hefei 230001, China; 2020146@glut.edu.cn

⁴ School of Material Science and Chemical Engineering, Anhui Jianzhu University, Hefei 230601, China; gaozhanzhang@126.com

⁵ Anhui Feitian New Material Technology Co., Ltd., Suzhou 234001, China; xwh891116@163.com

* Correspondence: 2021072@glut.edu.cn (W.X.); hucheng42@glut.edu.cn (C.H.)

Abstract: To prepare lightweight ultra high performance concretes used in the large-span and super-tall structure engineering fields, the effects of water-binder ratio on the mechanical performances, hydration products, and microstructure of the arched shell interface transition zone between the prewetting spherical lightweight aggregates and cement matrix were studied. The experimental results showed that adding prewetting spherical lightweight aggregates promoted the formation of an arched shell interface transition zone. And the hydration degree, microhardness, and elastic modulus values of the arched shell interface transition zone were still higher than the cement matrix. With the reduction of the water-binder ratio, the microhardness, elastic modulus, thickness, and compactness of the interface transition zone had an increase, and the internal curing action of the prewetting spherical lightweight aggregates was more obvious. Especially when the water-binder ratio was 0.18, the hydration degree of the arch shell interface transition zone increased by 18.27% compared with the cement matrix after 28 days curing time. It was concluded that the prewetting spherical lightweight aggregates could have better internal curing and arched shell effects in cement-based materials with a low water-binder ratio. Therefore, adding prewetting spherical lightweight aggregates was regarded as a potential measure to fabricate the lightweight ultra high performance concretes.

Keywords: prewetting spherical lightweight aggregates; arched shell interface transition zone; water-binder ratio; mechanical performances; microstructure



Citation: He, T.; Xiang, W.; Zhang, J.; Hu, C.; Zhang, G.; Kou, B. Influence of Water-Binder Ratio on the Mechanical Strength and Microstructure of Arch Shell Interface Transition Zone. *Buildings* **2022**, *12*, 491. <https://doi.org/10.3390/buildings12040491>

Academic Editors: Haoxin Li, Cong Ma and Tao Shi

Received: 4 March 2022

Accepted: 12 April 2022

Published: 15 April 2022

Publisher's Note: MDPI stays neutral with regard to jurisdictional claims in published maps and institutional affiliations.



Copyright: © 2022 by the authors. Licensee MDPI, Basel, Switzerland. This article is an open access article distributed under the terms and conditions of the Creative Commons Attribution (CC BY) license (<https://creativecommons.org/licenses/by/4.0/>).

1. Introduction

Ultra high-performance concrete (UHPC) with high mechanical properties and good durability has been widely used in urban overpasses, large bridges, marine engineering, and other fields [1,2]. However, due to the low water-binder ratio and large amount of cementing material, UHPC materials have some shortcomings, such as high apparent density (2600–2800 kg/m³), fast early hydration rate, large self-shrinkage, and so on. It leads the UHPC structure to be prone to shrinkage and cracking by the poor volume stability [3]. The shrinkage cracking of the concrete directly reduces its strength and durability, which will greatly shorten the service life of concrete members [4,5]. In addition, the external water is difficult to penetrate the UHPC owing to its dense structure. When the early curing stage is insufficient, the internal relative humidity of the concrete could decrease rapidly, resulting in the problems of early water loss and cracking of the concrete structure especially prominent [6]. It directly restricts the promotion and application of UHPC used in large-span and super-tall structure engineering.

Many researchers have tried to reduce the self-shrinkage and drying shrinkage of the UHPC materials by introducing shrinkage reducer, expansion agent, steel fiber, external

curing, and others [7,8]. Nevertheless, the shrinkage reducer has the problems of high price and reducing early strength of concrete [9]. The complementary shrinkage of the expansion agent consumes parts of water, which adversely affects the performance of cement-based materials with a low water-binder ratio [10]. Although steel fiber could reduce the self-shrinkage of concrete by its fiber toughening, the problem of high self-drying degree inside concrete is not solved [11]. External curing, such as coating organic solvent, sprinkling curing, and other methods, can not essentially solve the shrinkage and cracking caused by the insufficient internal humidity of concrete. Steam curing has the disadvantages of high production cost and large energy consumption [12]. Therefore, the methods to solve the problems of large bulk density and self-shrinkage cracking of lightweight ultra-high-performance concrete under the premise of guaranteeing high strength and excellent durability have become a hot topic in current research.

In recent years, some researchers like Cusson D [13], Ghourchian S [14], and Zhutovsky S [15] have found that the prewetting treatment of lightweight aggregates could continuously release water around in the process of concrete setting and hardening. It was beneficial to improve the internal relative humidity to reduce the shrinkage and cracking of the concrete materials. At the same time, the addition of prewetting lightweight aggregates promotes the formation of the interface transition zone between the lightweight aggregates and the cement matrix [16]. And the interface transition zone directly affects the physico-chemistry performances of the concrete [17,18]. Moreover, the high-performance, lightweight aggregates with 18.18% water absorption, 38.52% open porosity, 1.29 g/cm^{-3} apparent density, and 7.86 MPa cylinder compressive strength were prepared in our previous studies [19]. And then, our early experiment results showed that the internal curing action of prewetting spherical lightweight aggregates prompted the interface transition zone to form an arch shell structure, which was beneficial to evenly dispersing compressive stress to improve the strength of cement-based materials [20]. Therefore, it is inferred that the lightweight ultra high-performance concrete with low density, low shrinkage, ultra-high-strength, and high durability could be prepared using the internal curing and arch shell effects of prewetting spherical lightweight aggregates. At present, utilizing the prewetting spherical lightweight aggregates to replace parts of fine aggregates, the UHPC materials exceed 100 MPa compressive strength, $140\text{--}160 \times 10^{-6}$ autogenous shrinkage, and less than 2000 kg/m^3 apparent density after 28 days curing time were prepared by Liu Y [21] and Liu K [22]. The interface transition zone was regarded as an important factor affecting the physico-chemistry properties of the UHPC. However, not much literature has studied the performances and microstructure of the interface transition zone, which need to be further researched.

For preparing the lightweight ultra-high-performance concrete applied in the large-span and super-tall structure engineering, the effects of the water-binder ratio on the microhardness, elastic modulus, phase composition, micro-morphology, and microstructure parameters of C-S-H gel of the arched shell interface transition zone between the prewetting spherical lightweight aggregates and cement matrix were researched. The action mechanism of the water-binder ratio on mechanism performances and hydrate microstructure of the interface transition zone was discussed, which could lay a foundation for the preparation of lightweight ultra-high-performance concrete.

2. Experimental Programme

2.1. Raw Materials

In the study, the P.I 52.5 portland cement produced by Huaxin Cement Co., Ltd. was used as the cement raw material. Usually, the continuously graded aggregate mixtures have been used to prepare the UHPC materials to guarantee high packing. To verify the effect rule of the water-binder ratio on the interface transition zone, the size and type of aggregate in the study were not considered to simplify the experiment, and the particle size of aggregate was unchanged to $\Phi 2.35\text{--}4.75 \text{ mm}$ diameter size. And the high-performance spherical lightweight aggregates with 18.18% water absorption and 7.86 MPa cylinder compressive

strength prepared by our previous research were utilized as the internal curing agents. The polycarboxylene based superplasticizer with 25% solid content and 30% water reduction produced by Jiangsu Bote New Materials Co., Ltd. was used as the water reducer. The chemical compositions of the P.I 52.5 portland cement and high-performance, lightweight spherical aggregates are exhibited in Table 1. The physico-chemistry performances of the P.I 52.5 portland cement are shown in Table 2.

Table 1. The chemical compositions of the P.I 52.5 portland cement and high-performance spherical lightweight aggregates (wt%).

Raw Materials	SiO ₂	Al ₂ O ₃	Fe ₂ O ₃	CaO	MgO	K ₂ O	Na ₂ O	TiO ₂	SO ₃	Loss
Cement	20.87	4.87	3.59	64.47	2.13	0.65	0.11	0.97	0.77	1.31
Lightweight aggregates	47.98	23.41	8.67	12.96	1.02	1.68	1.31	0.90	0	1.08

Table 2. The physico-chemistry performances of the P.I 52.5 portland cement.

Specific Surface Area (m ² /kg)	Water Demand for Normal Consistency (%)	Compressive Strength (MPa)		Bending Strength (MPa)		Setting Time (min)		Weight of Screen Residue (%)	
		3 Days	28 Days	3 Days	28 Days	Initial Set	Final Set	80 μm	45 μm
369	27.2	32.1	58.8	6.1	9.6	128	185	0.5	0.5

2.2. Specimen Forming and Preparation

At first, the high-performance spherical lightweight aggregates were placed into 10 vol% red ink for 12 h prewetting processing and then were taken out, and their surfaces wiped of moisture. The subsequent water-binder ratios selected were 0.18, 0.20, and 0.22. The designed mix proportion of series B specimens is shown in Table 3. The gelled slurry was configured according to mix proportion and fully stirred by using a mortar mill and formed into 160 mm × 40 mm × 40 mm cuboid body and 40 mm × 40 mm × 40 mm cube body. Finally, the specimens were cured in a standard curing room with a 25 °C environment temperature and 95% RH curing humidity.

Table 3. The designed mix proportion of series B specimens.

Specimen No.	P.I 52.5 Portland Cement (kg/m ³)	Lightweight Aggregates (kg/m ³)	Water-Binder Ratio	Water Reducer (%)
B1	1029	596	0.18	2
B2	1029	596	0.20	2
B3	1029	596	0.22	2

Denoted by red ink, the internal curing range area of the prewetting spherical lightweight aggregates in the cement slurry with a low water-binder ratio was clearly observed, as shown in Figure 1. The arch shell interface transition zone, high-performance spherical lightweight aggregates, and cement matrix could be easily discerned by the red ink mark. As seen in Figure 1, RC was the lightweight aggregate, section B represented the cement matrix, section A represented the arch shell interface transition zone. After curing to the corresponding age, the section area containing lightweight aggregate, interface transition zone, and cement matrix of the specimen was selected by the high-speed cutter. The surface of the section area was polished to a mirror plane using diamond sand-paper, and it was used for the microhardness and microstructure test.

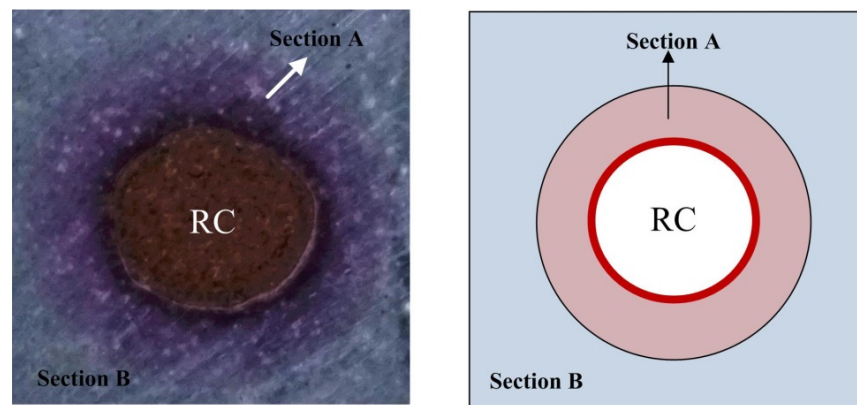


Figure 1. The internal curing range area of prewetting spherical lightweight aggregate in cement slurry with a low water-binder ratio.

2.3. Performance Testing

The microhardness of the interface transition zone was measured by the microhardness tester (HVS-1000, Lianer, Shanghai, China), and its test point method is shown in Figure 2. The elastic modulus of the specimen was measured by a nanoindentation instrument (Hysitron TI-980, Bruker, Ettlingen, Germany). The phase composition of the specimen was obtained by X-ray diffraction (XRD, PANalytical B.V., Almelo, The Netherlands) in the range of 10–80°. The hydration degree of the specimen and microstructure parameters of the hydration product C-S-H gel were characterized by the solid-state nuclear magnetic resonance spectrometer (NMR, Bruker 400 MHz, Faellanden, Switzerland) with the ^{29}Si NMR spectrum. The micro-morphology of the specimen was observed by field-emission scanning electron microscopy (FE-SEM, S4800, Hitachi, Tokyo, Japan).

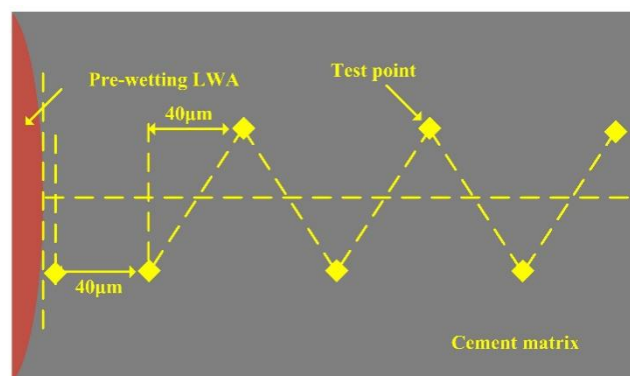


Figure 2. The microhardness test method of the interface transition zone.

3. Results and Discussion

The changes in the microhardness of the interface transition zone for specimens B1–B3 after 7 days and 28 days curing times are shown in Figure 3. It was seen that with the increase in the water-binder ratio the microhardness of the arch shell interface transition zone of specimens B1–B3 decreased gradually after curing at different ages, and the thickness of the arch shell interface transition zone decreased. When curing for 28 days, the microhardness values of specimens B1–B3 about 80 μm away from the surface of prewetting lightweight aggregates were 357.8 MPa, 321.6 MPa, and 266.4 MPa, respectively. Moreover, the microhardness of the arch shell interface transition zone was still higher than the cement matrix. This was mainly because the internal humidity of the cement paste gradually decreased during the hydration hardening, which formed the humidity difference between the pre-wetting lightweight aggregates and the hardening slurry, and the adsorbed water in the open pores of the pre-wetting lightweight aggregates

was gradually released under the capillary force action. It promoted the hydration of C_3S and C_2S in the surrounding slurry and increased the generation contents of C-S-H gel, Aft, and other hydration products, resulting in the improved compactness and mechanical performances of the arch shell interface transition zone.

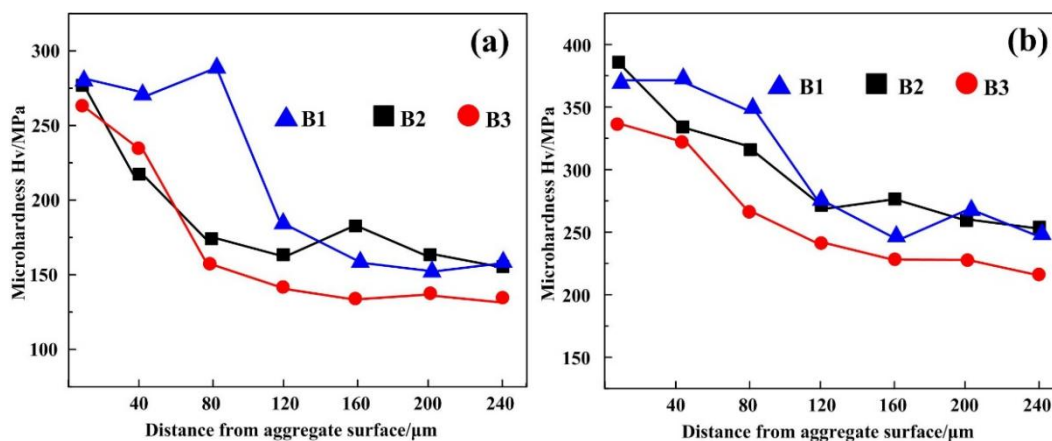


Figure 3. The changes of microhardness of the interface transition zone for specimens B1–B3 after 7 days and 28 days curing times. (a) 7 days curing time, (b) 28 days curing time.

When the water-binder ratio was lower, the humidity difference between the prewetting lightweight aggregates and the hardening slurry was more obvious during the hydration process. Meaning that the free water released from the prewetting lightweight aggregates had a faster migration rate in the slurry and a wider internal curing range. So the thickness of the arch shell interface transition zone increased, highlighting the interface effect between the lightweight aggregates and the cement matrix [23]. With the increase in the water-binder ratio, the compactness of the hardened slurry decreased, the size of internal pores increased, and the capillary force decreased. In the surrounding slurry, the migration rate of free water released by the internal curing action of the prewetting lightweight aggregates was slowed down, leading to a reduction in the thickness of the arch shell interface transition zone in specimens B2 and B3. At the same time, an increase in the water-binder ratio could significantly increase porosity inside the hardened slurry [24]. As a result, the microhardness of the cement matrix and the arch shell interface transition zone in specimens B2 and B3 were all less than specimen B1.

The change rule of elastic modulus of indentation points in specimen B1 after 28 days curing times was observed in Figure 4. As seen, the elastic modulus of lightweight aggregates was 30–60 GPa, the elastic modulus of cement matrix was 70–80 GPa, and the elastic modulus of the interface transition zone was 80–100 GPa. It was found that the elastic modulus of the interface transition zone was higher than the cement matrix. Moreover, the elastic modulus of the interface transition zone increased firstly. It then decreased with the increase of the distance from the aggregate surface, which conformed to the microhardness test results. Thereby, it was concluded that the internal curing action of the prewetting lightweight aggregates endowed the interface transition zone with the higher microhardness and elastic modulus, which contributed to preparing the ultra-high-performance concrete with low apparent density, low shrinkage, and high strength.

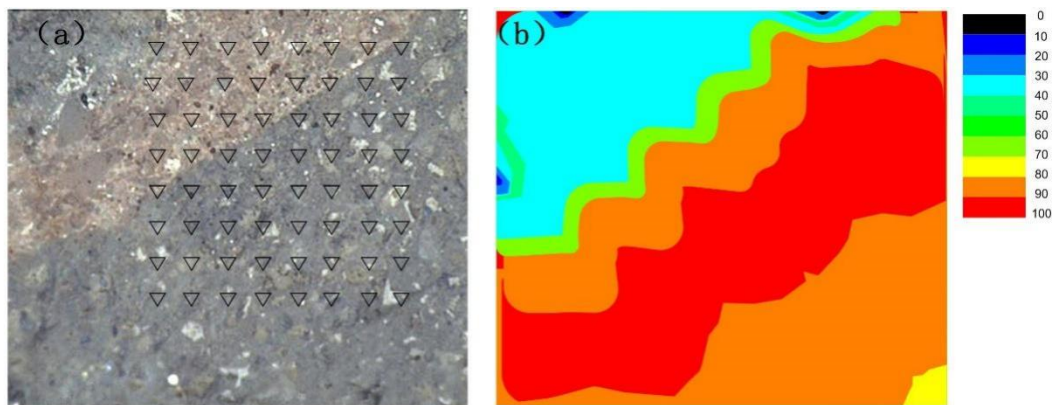


Figure 4. The change rule of elastic modulus of indentation points in specimen B1 after 28 days curing times (a) Indentation point distribution diagram, (b) Elastic modulus distribution nephogram.

To explore the effect mechanism of the water-binder ratio on the arched shell interface transition zone, the change rules of hydration products in the arched shell interface transition zone of series B specimens with different water-binder ratios were studied. The result is shown as follows.

The XRD patterns of cement matrix and interface transition zone of specimens B1–B3 after 28 days curing time were displayed in Figure 5. As seen in Figure 5a, it was seen that the major phase compositions of the cement matrix and interface transition zone of specimens B1–B3 all were C_3S , C_2S , CH, and AFt. When the water-binder ratio was 0.18, the generation content of hydration product CH was low, which indicated that the hydration degree of the cement matrix in the specimen was low. With the increase of the water-binder ratio, the characteristic peaks of C_3S and C_2S gradually weaken, while the characteristic peaks of CH and AFt gradually strengthen. This meant that the hydration degree of the cement matrix in series B specimens gradually increased with the increase of the water-binder ratio. Moreover, the characteristic peaks of hydration product CH in the interface transition zone of specimens B1–B3 increased compared with the cement matrix. It was regarded that the internal curing action of prewetting lightweight aggregates promoted the hydration and hardening of the arched shell interface transition zone.

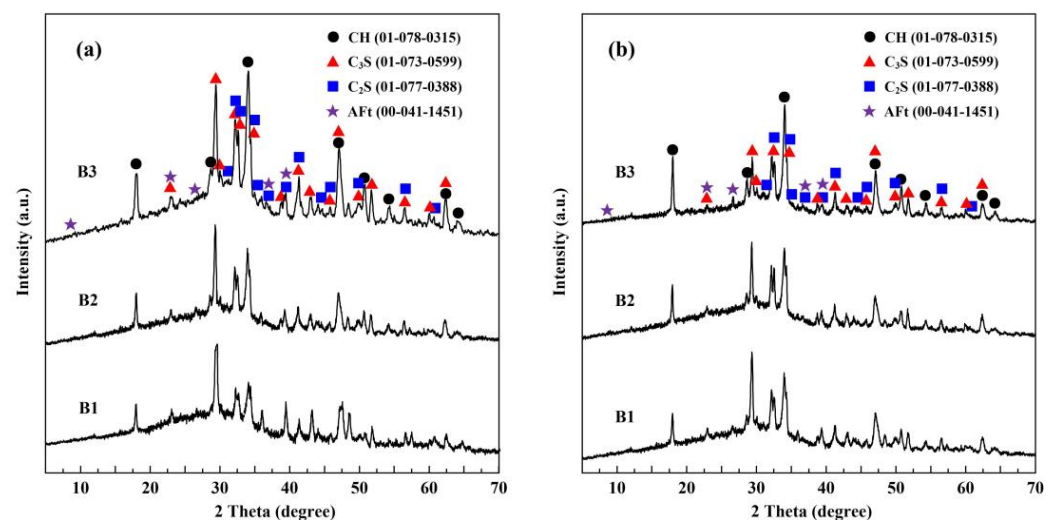


Figure 5. The XRD patterns of cement matrix and interface transition zone of specimens B1–B3 after 28 days curing time. (a) cement matrix, (b) interface transition zone.

To further reveal the influence of the water-binder ratio on the hydration products of the arched shell interface transition zone, the related microstructural parameters of

hydration product C-S-H gel in the cement matrix, and the interfacial transition zone of series B specimens were investigated.

The ^{29}Si NMR spectra of cement matrix of B-series sample after 28 days curing time were exhibited in Figure 6. After curing for 28 days, there were four spectral peaks in the cement matrix of the specimens B1–B3 between -60 ppm and -110 ppm, which represented the characteristic peaks of silicon-oxygen tetrahedron $[\text{SiO}_4]$ in the form of Q^0 , Q^1 , Q^2 (1Al) and Q^2 (0Al), respectively. Combined with the ^{29}Si NMR deconvolution results in Table 4, it was found that the peak intensities of Q^0 and Q^1 in the cement matrix gradually decreased with the increase of the water-binder ratio, while the total peak intensities of Q^2 (1Al) and Q^2 (0Al) had an increase. Moreover, the values of Q^2/Q^1 , MCL, and α_c gradually increased with the increase of the water-binder ratio. This was mainly caused by the free water content in the slurry, which increased via an increased water-binder ratio. It accelerated the hydration and hardening of cementitious materials, which promoted the formation of C-S-H gel with chain structure or ring structure.

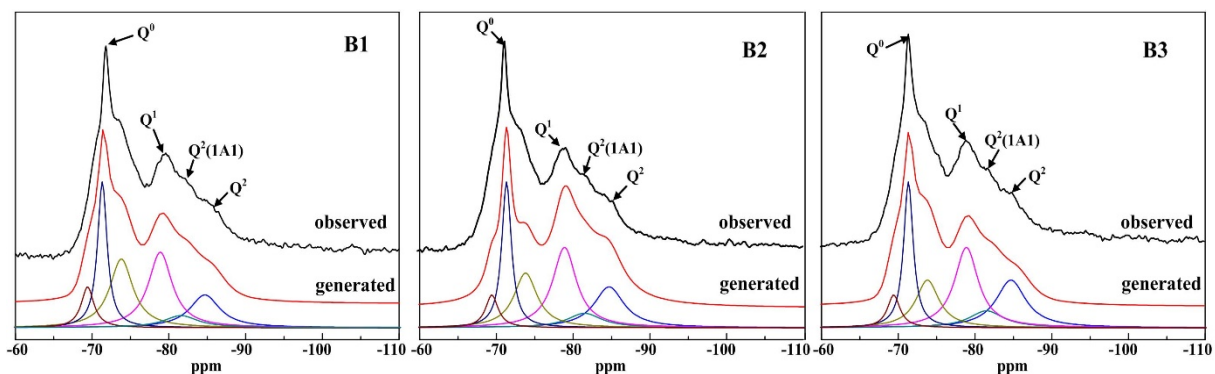


Figure 6. The ^{29}Si NMR spectra of cement matrix in specimens B1–B3 after 28 days curing time.

Table 4. The ^{29}Si NMR deconvolution results of cement matrix in specimens B1–B3 after 28 days curing time.

Sample No.	Water-Binder Ratio	Q^n				Q^2/Q^1	MCL	$\alpha_c/\%$
		Q^0	Q^1	Q^2 (1Al)	Q^2 (0Al)			
B1	0.18	52.76	33.71	4.29	9.24	0.40	2.93	47.24
B2	0.20	49.27	34.39	3.83	12.51	0.48	3.06	50.73
B3	0.22	47.91	33.72	4.16	14.21	0.54	3.21	52.09

The ^{29}Si NMR spectra of the arch shell interface transition zone in specimens B1–B3 after 28 days curing time were shown in Figure 7. It was seen that the silicon-oxygen tetrahedron $[\text{SiO}_4]$ of the arch shell interface transition zones in specimens B1–B3 after curing for 28 days mainly existed in the form of Q^0 , Q^1 , Q^2 (1Al), and Q^2 (0Al). Combined with the ^{29}Si NMR deconvolution results in Table 5, the hydration degrees of the arch shell interface transition zones in specimens B1–B3 after 28 days curing time were higher than the cement matrix.

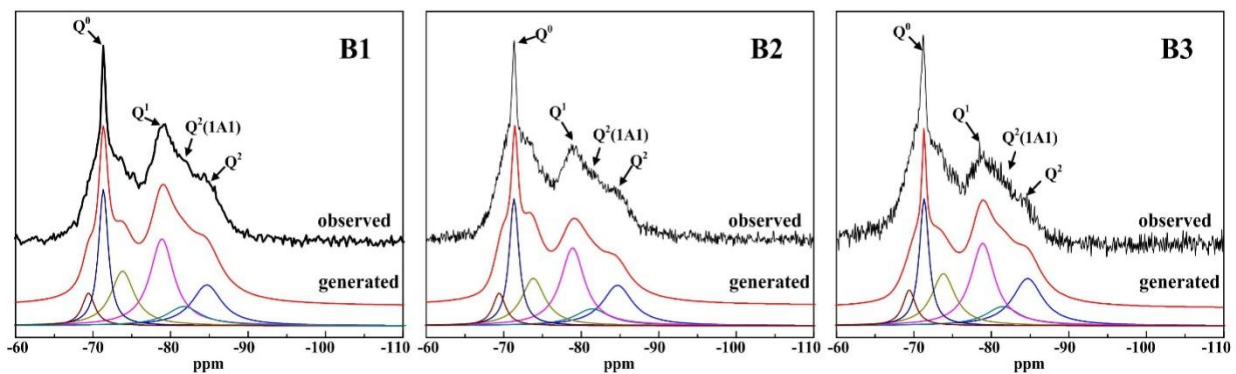


Figure 7. The ^{29}Si NMR spectra of arched shell interface transition zone in specimens B1–B3 after 28 days curing time.

Table 5. The ^{29}Si NMR deconvolution results of arched shell interface transition zone in specimens B1–B3 after 28 days curing time.

Sample No.	Water-Binder Ratio	Q^n				Q^2/Q^1	MCL	$\alpha_c/\%$
		Q^0	Q^1	Q^2 (1AI)	Q^2 (0AI)			
B1	0.18	44.13	35.17	4.19	16.51	0.59	3.30	55.87
B2	0.20	41.29	33.74	4.66	20.31	0.74	3.62	58.71
B3	0.22	40.13	34.69	3.22	21.96	0.73	3.54	59.87

Compared with the cement matrix, the hydration degree of the arch shell interface transition zones in specimens B1–B3 increased by 18.27%, 15.73%, and 14.94%, respectively. Therefore, it was concluded that the addition of prewetting spherical lightweight aggregates improved the hydration degree of the arch shell interface transition zone. This was because the internal curing behavior of the prewetting lightweight aggregates promoted the hydration of mineral phases C_3S and C_2S in the interface transition zone, which accelerated the formation of hydration products like C-S-H gel and Aft. In addition, with the increase in the water-binder ratio, the internal curing effect of prewetting lightweight aggregates gradually decreased, accompanied by the decrease of the hydration degree improvement trend of the arch shell interface transition zone. It was indicated that the prewetting spherical lightweight aggregates could have more obvious internal curing action to better promote the hydration of the interface transition zone under the condition of a low water-binder ratio.

The SEM images of the cement matrix of specimens B1–B3 after 28 days curing time are shown in Figure 8. When the water-binder ratio was from 0.18 to 0.22, the hydration products of the cement matrix in specimens B1–B3 were mainly fibrous or loccular C-S-H gel and laminar CH, and the laminar CH grains were cladding by the fibrous or loccular C-S-H gel. So the microstructure of the cement matrix was relatively dense. But meanwhile, some incomplete hydrated C_3S and C_2S grains still existed in the cement matrix, consistent with the XRD and ^{29}Si NMR analysis results. It was indicated that prolonging the curing time could further promote the hydration of the cement matrix and enhance the mechanical strength of the cement matrix. With the increase in the water-binder ratio, although the hydration degree of the cement matrix was improved, the compactness of the materials was reduced due to the existence of some pores. It caused the microhardness values of the cement matrix in specimens B1–B3 to decrease gradually with the increase in the water-binder ratio.

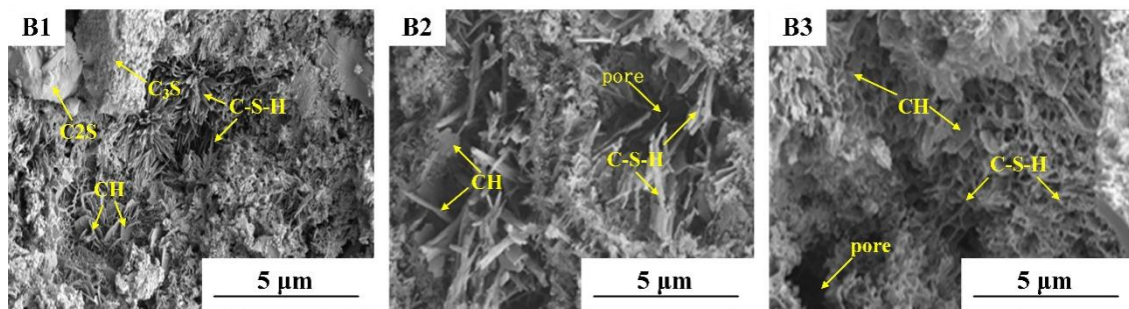


Figure 8. The SEM morphologies of cement matrix in specimens B1–B3 after 28 days curing time.

The low magnification SEM images of the arch shell interface transition zone in specimens B1–B3 after 28 days curing time are shown in Figure 9, and the high magnification SEM images of the arch shell interface transition zone in specimens B1–B3 after 28 days curing time are displayed in Figure 10. As seen in Figures 9 and 10, the cement matrix, arch shell interface transition zone, and lightweight aggregates were closely bonded in specimens B1–B3. The microstructure of the hardened slurry with a 0.18–0.22 water-binder ratio was relatively dense. At the same time, it was found that parts of fibrous or locular C-S-H gel in the arch shell interface transition zone filled the surface micropores of the lightweight aggregates, which was conducive to increasing the bonding properties between the interface transition zone and lightweight aggregates to improve the ability of cement-based materials to resist external loads [25,26]. However, with the increase in the water-binder ratio, the internal pores in the interfacial transition zone gradually increased, resulting in the compactness of the arch shell interfacial transition zone decreasing. Among these, some pores were clearly observed in the interface transition zone after curing for 28 days when the water-binder ratio increased to 0.22, and tiny gaps even appeared between the interfacial transition zone and the lightweight aggregates, which would cause an unfavorable influence on the mechanical strength of cement-based materials.

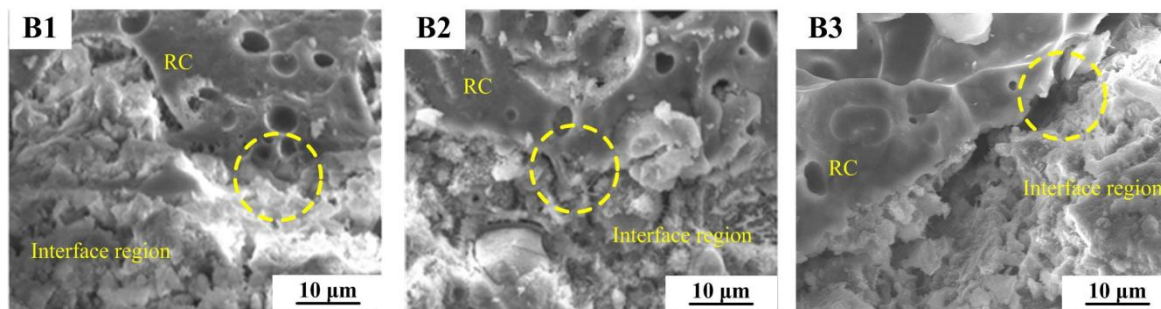


Figure 9. The low magnification SEM images of arched shell interface transition zone in specimens B1–B3 after 28 days curing time.

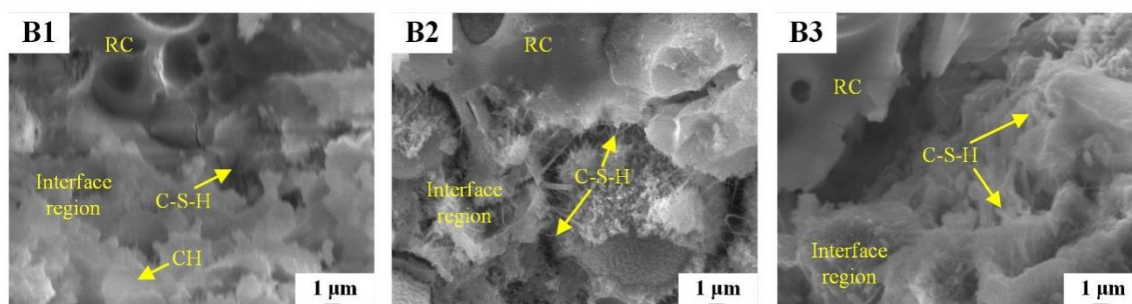


Figure 10. The high magnification SEM images of arched shell interface transition zone in specimens B1–B3 after 28 days curing time.

4. Conclusions

1. Compared with the cement matrix, the arched shell interface transition zone with higher microhardness and higher elastic modulus was formed by adding prewetting spherical lightweight aggregates. The microhardness and elastic modulus of the interface transition zone increased firstly and then decreased with an increase in distance from the lightweight aggregate surface.
2. The internal curing action of the prewetting spherical lightweight aggregates accelerated the hydration of its surrounding cement slurry. It promoted the generation of hydration products to improve compactness and mechanical performances of the arched shell interface transition zone, which was conducive to preparing lightweight ultra-high-performance concrete used in large-span and super-tall structure engineering.
3. The internal curing and arched shell effects of the prewetting spherical lightweight aggregates gradually increased with the reduction of the water-binder ratio. The internal curing action of the prewetting spherical lightweight aggregates was better with the addition of a 0.18 water-binder ratio. It caused the hydration degree of the arch shell interface transition zone to increase by 18.27% compared with the cement matrix after 28 days curing time.

Author Contributions: Data curation and analysis, T.H., W.X. and G.Z.; writing—original draft preparation, W.X.; writing—review editing, C.H., J.Z. and B.K. All authors have read and agreed to the published version of the manuscript.

Funding: The research was funded by the Guangxi Science Base and Talents Special Program (No.2021AC19047 and 2021AC19317), the National Science Natural Science Foundation of China (No.U21A20149 and No.51878003), and the Basic Ability Enhancement Program for Young and Middle-aged Teachers of Guangxi (No.2022KY0242 and 2021KY0262).

Institutional Review Board Statement: Not applicable.

Informed Consent Statement: Not applicable.

Data Availability Statement: The data presented in this study are provided by second author Weiheng Xiang.

Acknowledgments: The authors are grateful to the Guilin University of Technology for providing laboratory facilities and equipment.

Conflicts of Interest: The authors declare no conflict of interest.

References

1. Wang, X.; Yu, R.; Song, Q.; Shui, Z.; Liu, Z.; Wu, S.; Hou, D. Optimized design of ultra-high performance concrete (UHPC) with a high wet packing density. *Cem. Concr. Res.* **2019**, *126*, 105921. [[CrossRef](#)]
2. Shi, C.J.; Wu, Z.M.; Xiao, J.F. A review on ultra high performance concrete: Part I. raw materials and mixture design. *Constr. Build. Mater.* **2015**, *101*, 741–751. [[CrossRef](#)]
3. Zhang, X.; Liu, Z.; Wang, F. Autogenous shrinkage behavior of ultra-high performance concrete. *Constr. Build. Mater.* **2019**, *226*, 459–468. [[CrossRef](#)]
4. Meng, W.; Khayat, K.H. Effect of hybrid fibers on fresh properties, mechanical properties, and autogenous shrinkage of cost-effective UHPC. *J. Mater. Civ. Eng.* **2018**, *30*, 04018030. [[CrossRef](#)]
5. Mosaberpanah, M.A.; Eren, O.; Tarassoly, A.R. The effect of nano-silica and waste glass powder on mechanical, rheological, and shrinkage properties of UHPC using response surface methodology. *J. Mater. Res. Technol.* **2019**, *8*, 804–811. [[CrossRef](#)]
6. Shen, P.; Lu, L.; He, Y.; Rao, M.; Fu, Z.; Wang, F.; Hu, S. Experimental investigation on the autogenous shrinkage of steam cured ultra-high performance concrete. *Constr. Build. Mater.* **2018**, *162*, 512–522. [[CrossRef](#)]
7. Koh, K.; Ryu, G.; Kang, S.; Park, J.; Kim, S. Shrinkage properties of ultra-high performance concrete (UHPC). *Adv. Sci. Lett.* **2011**, *4*, 948–952. [[CrossRef](#)]
8. Huang, H.; Ye, G.; Fehling, E.; Middendorf, B.; Thiemicke, J. Use of rice husk ash for mitigating the autogenous shrinkage of cement pastes at low water cement ratio. In Proceedings of the HiPerMat 2016 4th International Symposium on Ultra-High Performance Concrete and High Performance Construction Materials, Kassel, Germany, 1 March 2016; pp. 9–11.
9. Zhu, Y.; Zhang, H.; Zhang, Z.; Yao, Y. Electrochemical impedance spectroscopy (EIS) of hydration process and drying shrinkage for cement paste with W/C of 0.25 affected by high range water reducer. *Constr. Build. Mater.* **2017**, *131*, 536–541. [[CrossRef](#)]

10. Bao, M.W.; Li, J.W.; Zain MF, M.; Lai, F.C. Development of soda residue concrete expansion agent. *J. Wuhan Univ. Technol.-Mater. Sci. Ed.* **2003**, *18*, 79–82.
11. Dügenci, O.; Haktanir, T.; Altun, F. Experimental research for the effect of high temperature on the mechanical properties of steel fiber-reinforced concrete. *Constr. Build. Mater.* **2015**, *75*, 82–88. [[CrossRef](#)]
12. Poovizhiselvi, M.; Karthik, D. Experimental Investigation of Self Curing Concrete. *Int. Res. J. Eng. Technol.* **2017**, *4*, 2395–0056.
13. Cusson, D.; Hoogeveen, T. Internal curing of high-performance concrete with pre-soaked fine lightweight aggregate for prevention of autogenous shrinkage cracking. *Cem. Concr. Res.* **2008**, *38*, 757–765. [[CrossRef](#)]
14. Ghourchian, S.; Wyrzykowski, M.; Lura, P.; Shekarchi, M.; Ahmadi, B. An investigation on the use of zeolite aggregates for internal curing of concrete. *Constr. Build. Mater.* **2013**, *40*, 135–144. [[CrossRef](#)]
15. Zhutovsky, S.; Kovler, K.; Bentur, A. Effect of hybrid curing on cracking potential of high-performance concrete. *Cem. Concr. Res.* **2013**, *54*, 36–42. [[CrossRef](#)]
16. Bentz, D.P.; Jensen, O.M. Mitigation strategies for autogenous shrinkage cracking. *Cem. Concr. Compos.* **2004**, *26*, 677–685. [[CrossRef](#)]
17. Zhutovsky, S.; Kovler, K.; Bentur, A. Influence of cement paste matrix properties on the autogenous curing of high-performance concrete. *Cem. Concr. Compos.* **2004**, *26*, 499–507. [[CrossRef](#)]
18. Bentz, D.P. Internal curing of high-performance blended cement mortars. *ACI Mater. J.* **2007**, *104*, 408–414.
19. Xiang, W.H.; Ding, Q.J.; Zhang, G.Z. Preparation and characterization of porous anorthite ceramics from red mud and fly ash. *Int. J. Appl. Ceram. Technol.* **2020**, *17*, 113–121. [[CrossRef](#)]
20. Ding, Q.J.; Xiang, W.H.; Zhang, G.Z.; Hu, C. Effect of prewetting lightweight aggregates on the mechanical performances and microstructure of cement pastes. *J. Wuhan Univ. Technol. Mater. Sci. Ed.* **2020**, *35*, 140–146. [[CrossRef](#)]
21. Liu, Y.; Wei, Y. Internal curing efficiency and key properties of UHPC influenced by dry or prewetted calcined bauxite aggregate with different particle size. *Constr. Build. Mater.* **2021**, *312*, 125406. [[CrossRef](#)]
22. Liu, K.; Yu, R.; Shui, Z.; Li, X.; Ling, X.; He, W.; Yi, S.; Wu, S. Effects of pumice-based porous material on hydration characteristics and persistent shrinkage of ultra-high performance concrete (UHPC). *Materials* **2018**, *12*, 11. [[CrossRef](#)] [[PubMed](#)]
23. Yang, C.C. Effect of the percolated interfacial transition zone on the chloride migration coefficient of cement-based materials. *Mater. Chem. Phys.* **2005**, *91*, 538–544. [[CrossRef](#)]
24. Asbridge, A.H.; Page, C.L.; Page, M.M. Effects of metakaolin, water/binder ratio and interfacial transition zones on the microhardness of cement mortars. *Cem. Concr. Res.* **2002**, *32*, 1365–1369. [[CrossRef](#)]
25. Kapeluszna, E.; Kotwica, Ł.; Różycka, A.; Gołek, Ł. Incorporation of Al in CASH gels with various Ca/Si and Al/Si ratio: Microstructural and structural characteristics with DTA/TG, XRD, FTIR and TEM analysis. *Constr. Build. Mater.* **2017**, *155*, 643–653. [[CrossRef](#)]
26. Liu, Q.; Shen, X.; Wei, L.; Dong, R.; Xue, H. Grey Model Research Based on the Pore Structure Fractal and Strength of NMR Aeolian Sand Lightweight Aggregate Concrete. *JOM* **2020**, *72*, 536–543. [[CrossRef](#)]